Electron-beam-induced deposition with carbon nanotube emitters

Lixin Dong, Fumihito Arai, and Toshio Fukuda[a)]
Department of Micro System Engineering, Nagoya University, Nagoya 464-8603, Japan

(Received 6 February 2002; accepted for publication 10 July 2002)

Electron-beam-induced deposition (EBID) is performed with multiwalled carbon nanotube emitters that are assembled to atomic force microscope cantilevers through nanorobotic manipulations. A typical experiment shows that under 120 V bias, field emission current 2 μA occurs from a nanotube emitter. In comparison with conventional EBID with a Schottky-type electron gun of a field-emission scanning electron microscope (FESEM) in the same vacuum chamber, the deposition rate of the nanotube emitter reaches up to 12.2% of that of FESEM although the bias and the emission current are only 0.8% and 1.9% of those of FESEM (15 kV and 106 μA). The concept of parallel EBID is also presented. © *2002 American Institute of Physics.* [DOI: 10.1063/1.1504486]

Electron-beam-induced deposition (EBID) is caused by the dissociation of molecules adsorbed to a surface by high-energy electrons, and has been demonstrated as an additive nanolithography[1] for many applications such as etch masks,[2,3] atomic force microscope (AFM) probe tips,[4–6] and other nanostructures.[7,8] However, low deposition rates and high cost obstacle its applications although its potential feature size can be smaller than its counterpart: focused ion beam deposition for the fabrication of 3D nanostructures. Although multiexposure electron beam[9] can improve its productivity, it provides no solution for the problem of cost because it still involves field-emission scanning electron microscope (FESEM) or similar equipments that equipped with expensive thermal electron filaments. Parallel EBID with cheaper field emitter array will be a synthetic solution for the above problem, but no work has been demonstrated so far.

On the other hand, carbon nanotubes (CNTs) have been demonstrated as well-defined cold cathodes,[10] because they can emit high current density under very low bias. Although intensive work has been done on the investigation of the field emission properties of CNTs[11] and their applications in flat display,[12] there has been no demonstration yet showing the feasibility of EBID with CNT emitters. Because of the possibility to fabricate well-aligned CNT arrays,[13,14] they may also find applications in parallel EBID, which will lead to broader application of EBID.

There have been some demonstrations on conventional 2D lithography by using CNT tips,[15,16] but as shown by Koops,[1] conventional lithography is not effective for the fabrication of 3D nanostructures.

In this letter, we show the feasibility of EBID through individual CNT emitters, and present parallel EBID with CNT arrays as a 3D large-scale nanofabrication technique.

The experiment system of CNT emitter for EBID is shown in Fig. 1, in which a CNT is mounted on an AFM cantilever and is placed above an Au-coated Si substrate. The CNT is used as cathode, while the substrate as anode. The gap L between the tip of the CNT and the substrate can be adjusted by mounting the cantilever and substrate onto unit 1 and unit 2 of the nanorobotic manipulation system[17,18] shown in Fig. 2, which also provides the possibility to generate a deposit pattern through EBID onto the substrate by servo control of the substrate, which is achieved by magnetic servo control of e beam in a conventional EBID system.

Nanorobotic manipulators provide the possibility to select CNTs with proper diameters so as to obtain high enough emission current, to assemble CNT electron emitters and to adjust the field by positioning the CNT above the substrate with a proper gap.

The nanorobotic manipulators are mounted inside a FESEM for obtaining real-time observation, for the preparation of CNT emitters, and for the comparison of EBID with CNT emitters and conventional EBID in the same circumstance.

A typical CNT emitter as shown in Fig. 3 is prepared through nanoassembly[18] of a multiwalled carbon nanotube (MWNT) onto a commercially available Au-coated Si_3N_4 AFM cantilever as field emitter. The inset shows the MWNT is mounted with conventional EBID deposit.

Typical precursors for EBID include WF_6, carbonyls, styrene, pump-oil, etc, and deposits are, respectively, W, metal carbides, carbonaceous, contamination, etc. Here we apply pump oil (chamber contamination) inside the FESEM to simplify the problem.

Figure 4(a) shows the configuration of the MWNT emitter and the substrate before EBID, where the dimensions of the MWNT are $\phi 28\ \text{nm} \times 2.7\ \mu\text{m}$ and the gap $L = 377$ nm. By applying a dc bias $V = 120$ V (field 318.3 V/μm) between the nanotube and the substrate, field emission current $I = 2\ \mu$A occurred (current density: 6.1×10^8 A/m^2). Figure 4(b) shows the deposit on the substrate after 20 min deposition. The height of the deposit is about 70 nm, and the diameter of the deposit is 204 nm. The growth rate R_T is calculated as 0.17 nm/s.

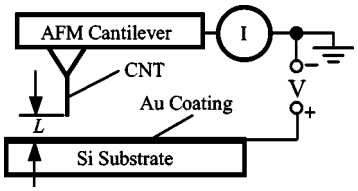

FIG. 1. Configuration of CNT-emitter EBID system.

a)Electronic mail: fukuda@mein.nagoya-u.ac.jp

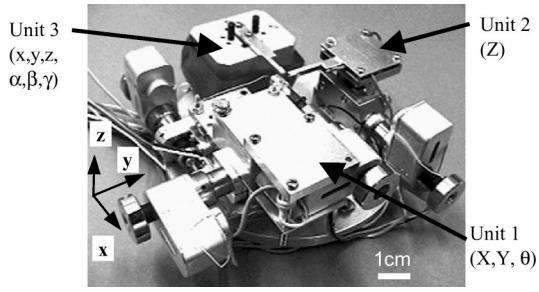

FIG. 2. Nanorobotic manipulators.

To compare the parameters with that of conventional EBID, an experiment is performed in the same vacuum chamber with the electron gun (Zr/O tungsten) of FESEM as shown in Fig. 5. The growth rate R_M can be obtained as 1.39 nm/s.

It can be found that the growth rate of EBID through the MWNT emitter reaches up to 12.2% of that of the conventional one, although the bias (120 V) and the emission current (2 μA) are only 0.8% and 1.9% of those of FESEM (15 kV and 106 μA), respectively. The way to improve growth rate further is discussed as follows.

According to the theoretical analyses by Koops,[2] the monolayer growth rate through EBID in equilibrium state is:

$$R = v \cdot N_O \cdot \frac{(g \cdot F/N_O) \cdot q \cdot f}{(g \cdot F/N_O) + 1/\tau + q \cdot f}, \tag{1}$$

where v is the volume occupied by a dissociated molecule or its fractions, N_o the molecule density in a monolayer, g the sticking coefficient, F the molecular flux density arriving on the substrate, q the cross section for dissociation of the adsorbed molecules under electron bombardment, f the electron flux density, and τ the lifetime of the molecules.

Note that the growth rate increases when the electron flux f and/or the molecular flux F are increased. In practice these parameters are limited, e.g., by electron optical constraints, the vapor supply and differential pumping system, or simply the fact that only a limited vapor pressure can be tolerated above the sample before significant electron scattering starts. Under these conditions, and note that the influence of the item including the lifetime τ of the molecules can be made negligible, e.g., by cooling the sample, the maximum rate obtainable for any given electron flux is

$$R_{\max} = v \cdot N_O \cdot q \cdot f, \tag{2}$$

and choosing

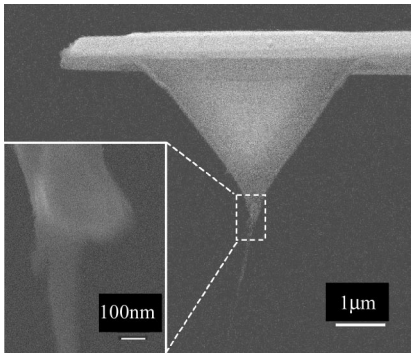

FIG. 3. CNT emitter (inset shows the EBID deposit).

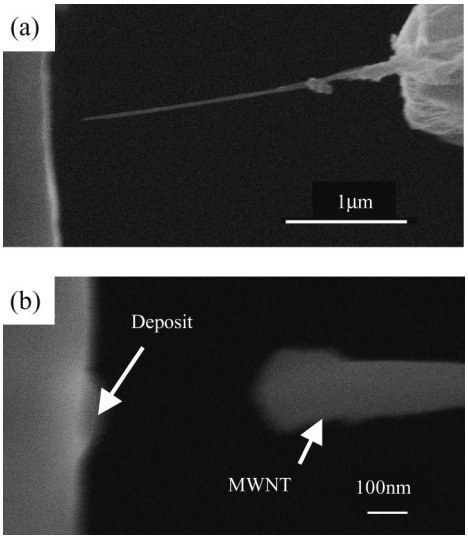

FIG. 4. EBID through MWNT electron emitter: (a) before EBID and (b) after EBID.

$$q \cdot f = g \cdot F/N_O \tag{3}$$

yields 50% of the maximum obtainable growth rate at supply F.

In the case of conventional EBID as shown in Fig. 5, $q = 2 \times 10^{-13}$ m^2 can be measured. Current density can be calculated as 5.3×10^{10} A/m^2, and hence the electron flux density of $f = 3.4 \times 10^{29}$ electrons/(m^2 s). In the same chamber, the molecular supply amount can be regarded unchanged by assuming $g = 1$. Hence, in the case of MWNT emitter as shown in Fig. 4, if the same growth rate is required, the electron flux density should be $f_{\mathrm{NT}} = 2 \times 10^{30}$ electrons/(m^2 s) noting that the $q_{\mathrm{NT}} = 3.3 \times 10^{-14}$ m^2. This suggests the current density is 3.2×10^{11} A/m^2, which is much larger than that obtained in the experiment 6.1×10^8 A/m^2. This gives the reason why the growth rate of the CNT emitter is lower than that of FESEM. To improve the growth rate, larger current and /or molecular flux are needed. The former can be realized by decreasing the gap size, increasing the applied bias, or using thinner CNTs. The latter can be improved by introducing gases into the specimen chamber but for completely resolving the later problem, parallel EBID with a CNT emitter array as shown in Fig. 6 will be an additional way.

In summary, electron-beam-induced deposition with an MWNT emitter has been observed. Under 120V bias, field emission current 2μA occurred from CNT emitter when the gap between the emitter and substrate was adjusted to be 377 nm. Although the bias and the emission current are only

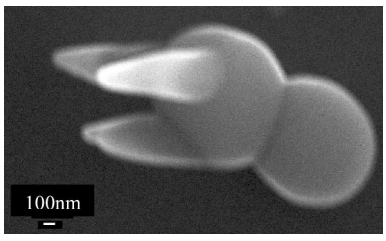

FIG. 5. EBID through conventional EBID (acceleration voltage: 15 kV, emitter current: 106 μA, deposition time: 3 min×4 times/finger, and base: ϕ1 μm polystyrene bead).

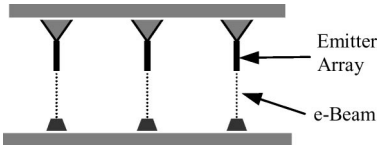

FIG. 6. Concept of parallel EBID.

0.8% and 1.9% of those of an FESEM (15 kV and 106 μA) emitter, respectively, the deposition rate reaches up to 12.2% of that of FESEM. Concept of parallel EBID through CNT-emitter array is presented, which is a promising way to realize large-scale fabrication of 3-D nanostructures.

This work was supported in part by the Scientific Research Fund of the Ministry of Education of Japan. We are grateful to Professor Y. Saito at Mie University for providing us with MWNT samples.

[1] H. W. P. Koops, J. Kretz, M. Rudolph, M. Weber, G. Dahm, and K. L. Lee, Jpn. J. Appl. Phys., **33-1**, 7099 (1994).
[2] H. W. P. Koops, R. Weiel, D. P. Kern, and T. H. Baum, J. Vac. Sci. Technol. B **6**, 477 (1988).
[3] A. N. Broers, Appl. Phys. Lett. **29**, 596 (1976).
[4] K. L. Lee and M. Hatzakis, J. Vac. Sci. Technol. B **7**, 1941 (1989).
[5] K. L. Lee, D. W. Abraham, F. Secord, and L. Landstein, J. Vac. Sci. Technol. B **9**, 3562 (1991).
[6] U. A. Griesinger, C. Kaden, N. Lichtenstein, J. Hommel, G. Lehr, R. Bergmann, A. Menschig, H. Schweitzer, H. Hillmer, H. W. P. Koops, J. Kretz, and M. Rudolph, J. Vac. Sci. Technol. B **11**, 2441 (1993).
[7] S. Matsui and K. Mori, J. Vac. Sci. Technol. B **4**, 299 (1986).
[8] S. Matsui, Proc. IEEE **85**, 629 (1997).
[9] S. Matsui, T. Kaito, J. I. Fujita, M. Komuro, K. Kanda, and Y. Haruyama, J. Vac. Sci. Technol. B **18**, 3181 (2000).
[10] I. Brodie, E. R. Westerberg, D. R. Cone, J. J. Muray, N. Williams, and L. Gasiorek, IEEE Trans. Electron Devices **28**, 1422 (1981).
[11] A. G. Rinzler, J. H. Hafner, P. Nikolaev, L. Lou, S. G. Kim, D. Tománek, P. Nordlander, D. T. Colbert, and R. E. Smalley, Science **269**, 1550 (1995).
[12] W. A. de Heer, A. Chatelain, and D. Ugarte, Science **270**, 1179 (1995).
[13] S. Fan, M. G. Chapline, N. R. Franklin, T. W. Tombler, A. M. Cassell, and H. J. Dai, Science **283**, 512 (1999).
[14] J. I. Sohn, S. Lee, Y.-H. Song, S.-Y. Choi, K.-I. Cho, and K.-S. Nam, Appl. Phys. Lett. **78**, 901 (2001).
[15] H. Dai, N. Franklin, and J. Han, Appl. Phys. Lett. **73**, 1508 (1998).
[16] A. Okazaki, T. Kishida, S. Akita, H. Nishijima, and Y. Nakayama, Jpn. J. Appl. Phys., Part 1 **39**, 7067 (2000).
[17] L. Dong, F. Arai, and T. Fukuda, J. Rob. Mech. **13**, 534 (2001).
[18] L. Dong, F. Arai, and T. Fukuda, *Proceedings of the 2001 IEEE International Conference on Robotics and Automation* (IEEE, Seoul, Korea, 2001), Vol. 1, pp. 632–637.